Experimental and Theoretical Study of the Hydride Migration to Ethylene in an Electron-Rich Cobalt Complex

Hubert Wadepohl,*,† Ute Kohl,† Maik Bittner,‡ and Horst Köppel*,‡

Anorganisch-Chemisches Institut der Ruprecht-Karls-Universität, Im Neuenheimer Feld 270, D-69120 Heidelberg, Germany, and Physikalisch-Chemisches Institut der Ruprecht-Karls-Universität, Theoretische Chemie, Im Neuenheimer Feld 229, D-69120 Heidelberg, Germany

Received November 26, 2004

The kinetics and energetics of β-migratory insertion in the electron-rich cobalt ethylene hydride complex $[(PMe_3)_3Co(H)(C_2H_4)]$ (**1**) were studied with experimental and theoretical techniques. The activation parameters were established in toluene solution using ^1H magnetization transfer methods. Data obtained over the temperature range 265−290 K gave $\Delta H^{\ddagger} = 16.4 \pm 0.6$ kcal mol^{-1} and $\Delta S^{\ddagger} = 8 \pm 2$ cal mol^{-1} K^{-1}. The structural and energetic parameters have also been determined by DFT electronic structure calculations. The global minimum thus obtained is in agreement with the experimental findings. The same holds true for the activation energies for migratory insertion as well as for β-elimination. Comparison of the activation parameters with those for other complexes suggests an increase of the barrier of migratory insertion with increasing electron richness of the metal center, which destabilizes species with agostic metal−H−C interactions. It is proposed that there may even be cases where an agostic structure is not an intermediate.

Introduction

So-called migratory insertion of an olefin into a metal−hydrogen bond and its microscopic reverse, β-hydrogen elimination, is a fundamental reaction in organometallic chemistry.[1] Both processes are key steps in many important catalytic cycles involving olefins.[2] For example, migratory insertions play a productive role in hydrogenation, isomerization, and hydroformylation reactions, to name just a few.[3] For olefin polymerization, β-elimination is a factor which limits the growth of the polymer chain. Numerous experimental and theoretical studies have been undertaken in order to understand these fundamental transformations.[4] The generally accepted mechanism is depicted in Scheme 1.

Certain restrictions are imposed onto the end points of the reaction, most importantly a cis stereochemistry of the hydride and olefin ligands in **A**[5] and a vacant two-electron coordination site as well as an available electron pair in **C**.[6]

Scheme 1

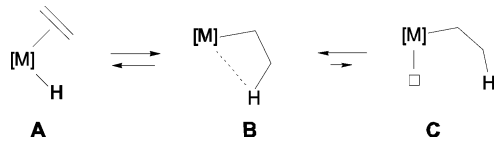

The coordinatively unsaturated alkyl complex **C** is generally assumed to be highest in energy. A considerable number of stable olefin hydride complexes **A** have been isolated; they represent the most common ground state of the system. In several cases, the β-agostic structure **B** could be directly or indirectly observed as a reactive intermediate, with an energy above that of the olefin hydride.[7] In a few cases, invariably with late transition metals, the agostic structure **B** has been found to be the most stable isomer.[8,9]

The kinetics of the β-elimination and migratory insertion processes have been examined previously for

† Anorganisch-Chemisches Institut.

‡ Physikalisch-Chemisches Institut.

(1) (a) Collman, J. P.; Hegedus, L. S.; Norton, J. R.; Finke, R. G. *Principles and Applications of Organotransition Metal Chemistry*; University Science Books: Mill Valley, CA, 1987. (b) Crabtree, R. H. *The Organometallic Chemistry of the Transition Metals*; Wiley: New York, 1988. (c) Elschenbroich, C. *Organometallchemie*, 4th ed.; Teubner: Stuttgart, Germany, 2003.

(2) Consiglio, G. *Chimia* **2001**, *55*, 809.

(3) Parshall, G. W.; Ittel, S. D. *Homegeneous Catalysis*, 2nd ed.; Wiley: New York, 1992.

(4) Comprehensive collections of relevant references may be found in: (a) Han, Y.; Deng, L.; Ziegler, T. *J. Am. Chem. Soc.* **1997**, *119*, 5939. (b) Vigalok, A.; Kraatz, H.-B.; Konstantinovsky, L.; Milstein, D. *Chem. Eur. J.* **1997**, *3*, 253. (c) Niu, S.; Hall, M. B. *Chem. Rev*. **2000**, *100*, 353.

(5) A special case of migratory insertion from a distorted trans configuration has been reported.[4b]

(6) (a) Reference 1b, p 42. (b) Lauher, J. W.; Hoffmann, R. *J. Am. Chem. Soc*. **1976**, *98*, 1729.

(7) See for example: (a) Kazlauskas, R. J.; Wrighton, M. S. *J. Am. Chem. Soc.* **1982**, *104*, 6005. (b) Yang, G. K.; Peters, K. S.; Vaida, V. *J. Am. Chem. Soc.* **1986**, *108*, 2511. (c) Derome, A. E.; Green, M. L. H.; Wong, L.-L. *New J. Chem*. **1989**, *13*, 747. (d) Johnson, F. P. A.; Gordon, C. M.; Hodges, P. M.; Poliakoff, M.; Turner, J. J. *J. Chem. Soc., Dalton Trans.* **1991**, 833.

(8) Co and Rh complexes: (a) Brookhart, M.; Green, M. L. H.; Pardy, R. B. A. *J. Chem. Soc., Chem. Commun*. **1983**, 691. (b) Cracknell, R. B.; Orpen, A. G.; Spencer, J. L. *J. Chem. Soc., Chem. Commun*. **1984**, 326. (c) Schmidt, G. F.; Brookhart, M. *J. Am. Chem. Soc*. **1985**, *107*, 1443. (d) Cracknell, R. B.; Orpen, A. G.; Spencer, J. L. *J. Chem. Soc., Chem. Commun*. **1986**, 1005. (e) Brookhart, M.; Lincoln, D. M.; Volpe, A. F., Jr.; Schmidt, G. F. *Organometallics* **1989**, *8*, 1212. (f) Brookhart, M.; Lincoln, D. M.; Bennett, M. A.; Pelling, S. *J. Am. Chem. Soc*. **1990**, *112*, 2691. (g) Brookhart, M.; Hauptmann, E.; Lincoln, D. M. *J. Am. Chem. Soc*. **1992**, *114*, 10394. (h) Daugulis, O.; Brookhart, M.; White, P. S. *Organometallics* **2003**, *22*, 4699.

10.1021/om0490740 CCC: $30.25
Publication on Web 03/22/2005

Table 1. NMR Data (δ, in Toluene-d_8) for [$(PMe_3)_3Co(H)(C_2H_4)$] (1)

nucleus, temp	hydride	C_2H_4	PMe_3
^{1}H, ambient	−20.42 (s, br, 1H)	1.78 (s, br, 4H)	1.08 (d, 27H), J(H,P) = 2.5 Hz
^{1}H, 190 K	−20.46 (dt, 1H), J(H,P) = 102 Hz (d), 68 Hz (t)	2.23 (br, 2H); 1.45 (br, 2H)	1.12 (s, br, 18H); 0.59 (s, br, 9H)
^{13}C, ambient		27.2 (br)	23.0 (br)
^{13}C, 190 K		26.7 (br)	25.3 (m), J(C,P) = 17 Hz, J(P,P) ≈ 500 Hz; 17.6 (d), J(C,P) = 17 Hz
^{31}P, ambient			8.7 (s, br)
^{31}P, 190 K			15.1 (s, $2P_{eq}$); 8.7 (s, $1P_{ax}$)

quite a few cases. However, apart from the somewhat vague statement of elimination being faster and migratory insertion being slower with the late transition metals[4a] (i.e. perhaps at the more electron rich metal centers) little generalization can be drawn from the available data. Although catalytic polymerization of ethylene by late-transition-metal complexes had been demonstrated already more than 20 years ago,[10] this process was believed to be severely limited by rapid β-hydrogen elimination on such metal centers. More recently it has been demonstrated that the chain transfer processes caused by β-hydrogen elimination[11] can be overcome by specially tailored catalysts, usually with bulky ligands, and that the facile elimination process can even be utilized to generate novel varieties of "hyperbranched" polymers with high molecular weight.[8h,9c,g,10c−e] It is obvious that the interplay between alkyl migration (chain growth) and β-hydrogen elimination/reinsertion determines the molecular weight and structure of the polymers.

Little data exist that allow a comparison of the energy barrier for the migratory insertion between the lighter and heavier metals within a group in the transition-metal series. A more detailed experimental study of a series of complexes of cobalt[8e] and rhodium[8g] seems to indicate a lower barrier ($\Delta H^{\ddagger}$) for cobalt than for rhodium. However, for the cobalt complexes the relevant activation barrier could only be estimated with considerable uncertainty, due to the β-agostic ground states of these systems. The same problem exists for some nickel and palladium complexes, where activation parameters ($\Delta H^{\ddagger}$ and/or $\Delta G^{\ddagger}$) for the β-hydrogen elimination/reinsertion process have been reported.[9e,f,i]

It is interesting to note that most of the available kinetic data were obtained with cationic systems, as are the above-mentioned polymerization catalysts. The present study aims at the ethylene migratory insertion−β-hydrogen elimination process in a neutral, electron-rich transition-metal system. For the cobalt ethylene hydride complex [$(PMe_3)_3Co(H)(C_2H_4)$] (**1**) we report experimental kinetic data for the migratory insertion (i.e. the hydride migration process). Theoretical calculations serve to obtain an energy profile for the reaction and establish intermediates and transition states.

Results and Discussion

Structure and Dynamic Behavior of [$(PMe_3)_3Co(H)(C_2H_4)$] (1). Complex **1** was obtained by protonation with methanol of the anion $[(PMe)_3Co(C_2H_4)]^-$.[12] The variable-temperature ^{1}H, ^{13}C, and ^{31}P NMR spectra (Table 1) reveal a pronounced stereochemical nonrigidity. Only broad resonances are observed at ambient temperature. At 190 K the resonances are of more diagnostic value. A 2:1 pattern with no apparent ^{31}P−^{31}P coupling is observed in the ^{31}P NMR spectrum. The hydride resonance is split into a doublet of triplets. The ethylene gives rise to a set of two somewhat broadened resonances in the ^{1}H spectrum, while only one carbon resonance can be assigned to this ligand. Further resonances appear for the methyl groups of the phosphine ligands; one of them has the typical appearance of virtual coupling (Table 1).

For a pentacoordinated complex, dynamic behavior is not surprising. In their original paper,[12] Klein et al. proposed structure **1D** based on a trigonal bipyramid, with an axial hydrido ligand and the ethylene in the equatorial position.[13] It was noted, however, that the

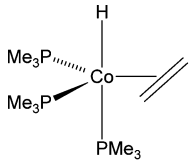

1, D

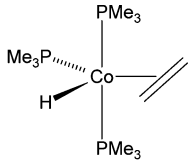

1, E

axial position of the hydride could not be deduced directly from the NMR spectra; assignment of the structure was made in analogy to that of [$(PMe_3)_3Co$-

(9) Ni, Pd, and Pt complexes: (a) Conroy-Lewis, F. M.; Mole, L.; Redhouse, A. D.; Litster, S. A.; Spencer, J. L. *J. Chem. Soc., Chem. Commun*. **1991**, 1601. (b) Carr, N.; Mole, L.; Orpen, A. G.; Spencer, J. L. *Organometallics* **1991**, *10*, 49. Carr, N.; Mole, L.; Orpen, A. G.; Spencer, J. L. *J. Chem. Soc., Dalton Trans*. **1992**, 2653. (c) Tempel, D. J.; Johnson, L. K.; Huff, R. L.; White, P. S.; Brookhart, M. *J. Am. Chem. Soc.* **2000**, *122*, 6686. (d) Younkin, T. R.; Connor, E. F.; Henderson, J. I.; Friedrich, S. K.; Grubbs, R. H.; Bansleben, D. A. *Science* **2000**, *287*, 460. (e) Shultz, L. H.; Brookhart, M. *Organometallics* **2001**, *20*, 3975. (f) Shultz, L. H.; Tempel, D. J.; Brookhart, M. *J. Am. Chem. Soc.* **2001**, *123*, 11539. (g) Ledford, J.; Shultz, C. S.; Gates, D. P.; White, P. S.; DeSimone, J. M.; Brookhart, M. *Organometallics* **2001**, *20*, 5266. (h) Connor, E. F.; Younkin, T. R.; Henderson, J. I.; Hwang, S. J.; Roberts, W. P.; Litzau, J. J.; Grubbs, R. H. *J. Polym. Sci. A1* **2002**, *40*, 2842. (i) Leatherman, M. D.; Svejda, S. A.; Johnson, L. K.; Brookhart, M. *J. Am. Chem. Soc*. **2003**, *125*, 3068. (j) Connor, E. F.; Younkin, T. R.; Henderson, J. I.; Waltman, A. W.; Grubbs, R. H. *Chem. Commun*. **2003**, 2272.

(10) Review articles: (a) Wilke, G. *Angew. Chem*. **1988**, *100*, 189. (b) Keim, W. *Angew. Chem*. **1990**, *102*, 251. (c) Guan, Z.; Cotts, P. M.; McCord, E. F.; McLain, S. J. *Science* **1999**, *283*, 2059. (d) Ittel, S. D.; Johnson, L. K.; Brookhart, M. *Chem. Rev.* **2000**, *100*, 1169. (e) Mecking, S. *Angew. Chem.* **2001**, *113*, 550.

(11) Direct β-hydrogen transfer to the coordinated monomer is also a possibility for chain transfer: (a) Stehling, U.; Diebold, J.; Kirsten, R.; Röll, W.; Brintzinger, H. H.; Jüngling, S.; Mülhaupt, R.; Langhauser, F. *Organometallics* **1994**, *13*, 964. (b) Gates, D. P.; Svejda, S. A.; Onate, E.; Killian, C. M.; Johnson, L. K.; White, P. S.; Brookhart, M. *Macromolecules* **2000**, *33*, 2320 and references therein.

(12) Klein, H.-F.; Hammer, R.; Gross, J.; Schubert, U. *Angew. Chem*. **1980**, *92*, 835.

(13) Throughout this paper we follow the conventional nomenclature for pentacoordinated structures (cf.: Albright, T. A.; Burdett, J. K.; Whangbo, M.-H. *Orbital Interactions in Chemistry*; Wiley: New York, 1985; Chapter 17). ax and eq refer to the axial and equatorial sites. For the ethylene ligand, the orientation with respect to the (pseudo) C_3 axis is denoted by ∥ (parallel) and ⊥ (perpendicular).

$(C_2H_4)CH_3]$,[13] which in turn was based on a comparison of the spectra with those of $[(PMe_3)_4Co(CH_3)]$.[14]

On the basis of the arguments put forward by Rossi and Hoffmann in their seminal paper on pentacoordination[15] structure **1D** is indeed the most likely candidate. However, preliminary DFT MO calculations indicated **1E** (H eq; C_2H_4 eq, $\perp$) to be of comparable energy.

The observed coupling pattern of the hydride NMR resonance at low temperature allows us to rule out several alternatives. In a structure with both the hydride and ethylene ligands in axial sites, the three ^{31}P nuclei would be equivalent, in contrast to our low-temperature spectra. The observed larger coupling of the hydride to one phosphorus ($J(^1H,^{31}P) = 102$ Hz) and smaller couplings to two such nuclei ($J(^1H,^{31}P) = 68$ Hz) also disfavors a structure with ethylene in the axial and the hydride in an equatorial position, where the reverse coupling pattern is expected. We can also rule out most of the possible structures based on the tetragonal pyramid, i.e. the ones with H apical, C_2H_4 basal, and the H and C_2H_4 both basal in a trans arrangement (three approximately equal couplings H, P expected). The number of possible structures can be further reduced when the temperature dependence of the resonances of the ethylene ligand is taken into account. At low temperature, two ^1H and one ^{13}C resonance are observed. This is only consistent with one of the remaining two likely candidates, namely **1D** (H ax, C_2H_4 eq, $\perp$), but not with **1E**.

Consistent with this reasoning our DFT MO calculations also favor **1D** with respect to **1E** (vide infra). We note that the phenyl derivative of **1**, $[(PMe_3)_3Co(Ph)(C_2H_4)]$ (**2**), has been shown by a crystal structure determination to adopt a structure analogous to **1E** (phenyl eq, C_2H_4 eq, $\perp$).[16] However, due to the low energy barriers between the many possible conformations of these systems, the assignment of the ground-state structure is of limited value for the comparatively high energy dynamic process (i.e. migratory insertion) pertinent to this study.

The dynamic behavior of **1** in solution can be described in terms of three different processes (Scheme 1). Process I is the scrambling of the ligands over all

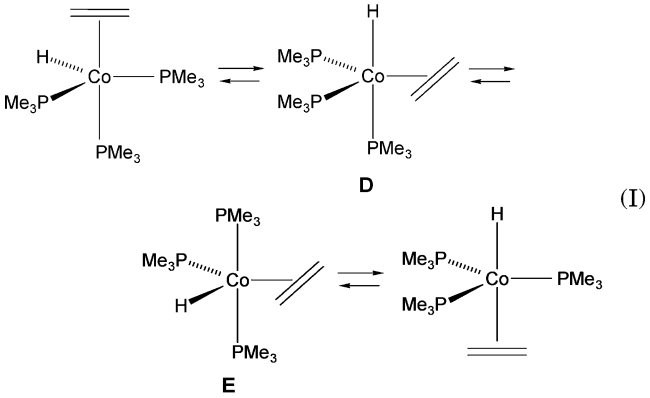

(I)

the sites in the five-coordinated complexes. Berry pseudorotation[17] is assumed to be the most probable rearrangement mechanism for trigonal-bipyramidal molecules[18] and is also likely operative in process I. In the ^{31}P NMR spectra process I results in the coalescence of the two resonances expected (and found at low temperature) for the ground-state structure **1D** into one single line at the fast exchange limit. It will also average out the two different couplings $^2J(^1H,^{31}P)$ of the hydride resonance. No attempt was made to fully quantify the energetics of this process experimentally. A rough estimation from the coalescence of the ^{31}P NMR resonances gives about 11 kcal mol^{-1} for the activation barrier.[19]

Process II is the rotation of the ethylene which exchanges the two CH_2 termini of this ligand. It can

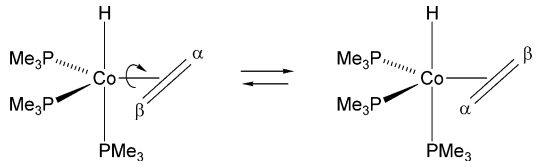

(II)

occur in any of the various conformational isomers generated by process I. We note here that the slow exchange limit for processes I and II (and also III, vide infra) is approached at 190 K. In addition, only one isomer, namely **1D**, is populated at that temperature. This gives a lower limit for the free enthalpy difference (ΔG^0) between the two most stable conformers of about 1 kcal mol^{-1}.

The hydride migration process III is slowest. The

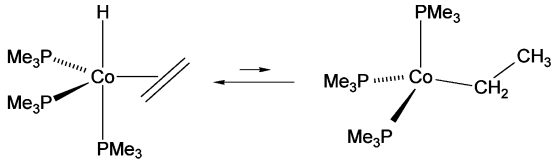

(III)

equilibrium concentration(s) of the "olefin inserted" products (with an agostic and/or free ethyl group, respectively) are too small to be observed by NMR spectroscopy. However, in combination with the generally faster process II (olefin rotation) complete scrambling of the five involved hydrogen atoms occurs. This has indeed been observed by Klein et al. in a deuteration experiment.[12]

Experimental Determination of the Activation Barrier for the Hydride Migration. In principle, rates for β-migratory insertion could be measured by a line shape analysis of the hydride resonance, since this is a process that results in an essential suppression of the $^1H-^{31}P$ spin−spin coupling, which is much smaller (essentially nonobservable in the present case) for the olefinic sites. In the present case, the shape of the hydride resonance is, however, also strongly affected by process I, which averages the coupling to the phosphorus nuclei, as described above. The effects of the two processes on the band shape cannot be separated.

(14) Klein, H.-F.; Karsch, H. H. *Chem. Ber.* **1975**, *108*, 944.
(15) Rossi, A. R.; Hoffmann, R. *Inorg. Chem.* **1975**, *14*, 365.
(16) Klein, H.-F.; Gross, J.; Hammer, R.; Schubert, U. *Chem. Ber.* **1983**, *116*, 1441.
(17) Berry, R. S. *J. Chem. Phys.* **1960**, *32*, 933.
(18) Jesson, J. P.; Muetterties, E. L. In *Dynamic Nuclear Magnetic Resonance Spectroscopy*; Jackman, L. M., Cotton, F. A., Eds.; Academic Press: New York, 1975; Chapter 8.
(19) Reaction rates and activation barriers based on the coalescence of singlets are notoriously error prone, due to a strong correlation of line width and exchange frequency. See e.g.: Binsch, G.; Kessler, H. *Angew. Chem.* **1980**, *92*, 445.

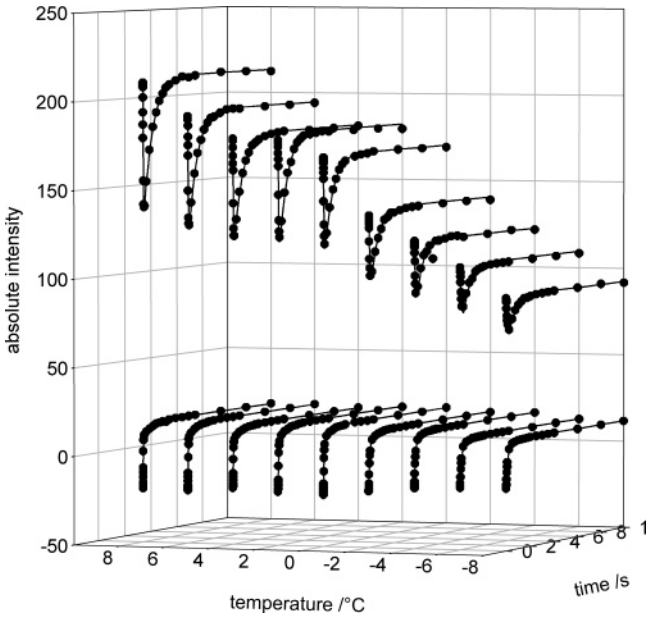

Figure 1. Time evolution of magnetization in the two sites (top traces, hydride resonance; bottom traces, ethylene resonance) after selective inversion of the hydride resonance. Data are shown in a pseudo-3D representation as a function of temperature.

We therefore resorted to magnetization transfer (MT) experiments, which are able to directly monitor the migration of the protons between the two sites (hydridic and olefinic) involved.[20] The technical problems that go along with the selective excitation of broad resonances can be overcome by modern techniques using shaped pulses.[21]

The usable temperature range of magnetization transfer experiments is intrinsically limited by T_1 relaxation and can be a major drawback for quantitative work.[22] This mainly affects the accuracy of activation entropy data extracted from MT data. In the present case, the low end of the temperature range was further limited by the onset of changes in the spectra due to the slowdown of the various conformational rearrangements. In a series of complementary experiments carried out with **1** in a toluene-d_8 solution between −10 and +10 °C, the ethylene or hydride resonances, respectively, were selectively inverted with a shaped pulse, followed by monitoring of the time evolution of the intensities in the respective sites. The results of experiments in which magnetization at the hydridic site was inverted are shown in Figure 1.

For any temperature T, the time dependence of the magnetization in either of the two sites (the previously inverted site and the one connected to it by chemical exchange) can be derived directly from the McConnell equations[23] for exchange between two sites.[24] Numerical nonlinear least-squares fits of the theoretical curves to the experimental data gave, among other quantities such as relaxation rates, the NMR spectroscopic rate constants $k_{\mathrm{NMR,ins}}(T)$ for the hydride migration. The kinetic information acquired from the two complementary experiments is strictly redundant.[25] Any discrepancies are due to systematic and random errors in the experiments. Although each series was also analyzed separately, we took the conservative approach of using redundant data (a combination of the two series of experiments; see the last column in Tables 2 and 3) to obtain what we believe to be the most realistic activation parameters.

Table 2. Rate Constants $k_{\mathrm{chem,ins}}$ (s^{-1}) for the Migratory Insertion Process in Complex 1[a]

temp (K)	hydride inversion	ethylene inversion	combined data
267	7.6(3)		
269	11.9(4)	14.7(2)	12.46(7)
271	15.4(4)	18.8(1)	18.0(2)
273	15.6(3)	21.2(1)	19.89(6)
275	20.7(5)	26.7(7)	23.5(2)
277	30.1(3)	33.0(2)	32.0(1)
279	34.2(6)	41.3(3)	41.7(1)
281	38.7(7)	53.1(2)	48.2(1)
283	52.7(1)	65.3(3)	63.9(2)
285		78.6(4)	

[a] Numbers in parentheses are the standard errors from the nonlinear least-squares analyses.

Table 3. Activation Parameters ($\Delta H^{\ddagger}$ and $\Delta G^{\ddagger}$ in kcal mol^{-1}, $\Delta S^{\ddagger}$ in cal mol^{-1} K^{-1}) for β-Migratory Insertion in Complex 1

	hydride inversion	ethylene inversion	combined data
$\Delta H^{\ddagger}$	16.4 ± 1.0	15.6 ± 0.4	16.4 ± 0.6
$\Delta S^{\ddagger}$	7.2 ± 3.5	5.0 ± 1.3	7.7 ± 2.3
$\Delta G^{\ddagger}$(271 K)	14.4 ± 1.3	14.3 ± 0.5	14.3 ± 0.9

Taking into account the statistical factors for the forward and back reactions into and out of the respective sites,[26] $k_{\mathrm{NMR,ins}}(T)$ was then converted into the chemical rate constant $k_{\mathrm{chem,ins}}(T)$ (Table 2). Eyring plots[27] of $\ln[k_{\mathrm{chem,ins}}(T)hk_{\mathrm{B}}{}^{-1}T^{-1}]$ vs T^{-1} were used to calculate the activation parameters. The Eyring plot resulting from k values obtained from the simultaneous fit of data obtained from inversion of either site is shown in Figure 2. The analysis gave an enthalpy of activation for the hydrogen migration of $\Delta H^{\ddagger} = 16.4 \pm 0.6$ kcal mol^{-1} and a positive entropy of activation $\Delta S^{\ddagger} = 8 \pm 2$ cal mol^{-1} K^{-1}. Table 4 gives a comparison of our activation parameters for the hydride migration with data taken from the literature for related complexes.

Electronic Structure Calculations. To gain further insight into the various stationary points and reaction pathways, electronic structure calculations have been carried out. Full geometry optimizations were performed, starting from the two most likely pseudo-trigonal-bipyramidal candidates for the ground state of **1**: (i) axial hydrogen with ethylene equatorial and oriented perpendicular to the pseudo-C_3 axis of the system (structure **1D** depicted in Figure 3a) and (ii) equatorial hydrogen with ethylene equatorial and oriented perpendicular to the pseudo-C_3 axis (structure **1E** depicted in Figure 4a).

(20) Forsén, S.; Hoffman, R. A. *J. Chem. Phys.* **1963**, *39*, 2892; **1966**, *45*, 2049.
(21) Kessler, H.; Mronga, S.; Gemmecker, G. *Magn. Reson. Chem.* **1991**, *29*, 527.
(22) Orrell, K. G.; Šik, V.; Stephenson, D. *Prog. NMR Spectrosc.* **1990**, *22*, 141.
(23) McConnell, H. M. *J. Chem. Phys.* **1958**, *28*, 430.
(24) (a) Leigh, J. S. *J. Magn. Reson.* **1971**, *4*, 308. (b) Campbell, I. D.; Dobson, C. M.; Ratcliffe, R. G.; Williams, R. J. P. *J. Magn. Reson.* **1978**, *29*, 397. (c) Led, J. J.; Gesmar, H. *J. Magn. Reson.* **1982**, *49*, 444.
(25) This only holds true under certain conditions (notably complete inversion of the respective resonances), which were fulfilled in our experiments.
(26) Green, M. L. H.; Wong, L.-L.; Sella, A. *Organometallics* **1992**, *11*, 2660.
(27) Laidler, K. J. *Reaktionskinetik I*; Bibliographisches Institut: Mannheim, Germany, 1970.

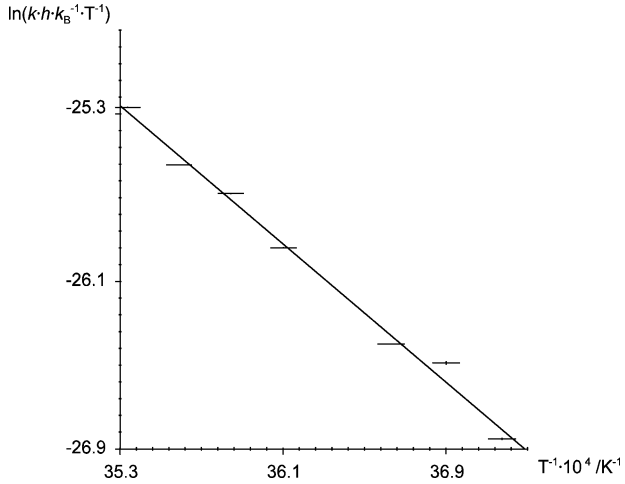

Figure 2. Eyring plot for the data from the last column of Table 2.

Key geometric parameters for the optimized structures are collected in Table 5. We found considerable deviations from the idealized pseudo-bipyramidal geometry. First, the pseudo-C_3 axis is not exactly linear. Second, the equatorial plane is not exactly planar. Third, the angles between the ligands in the equatorial plane are not 120°. These deviations result from the attachment of ethylene and the large spatial extension of the ligands.

Structural Parameters of the Stationary Points. Structure **1D** (Figure 3a) represents the global minimum of the part of the potential energy surface investigated. Structure **1E** (Figure 4a) lies 3.6 kcal mol^{-1} higher than the global minimum. From each of the ethylene structures a simple migration of the hydride ligand to one carbon terminus of the coordinated ethylene leads to the corresponding ethyl structures (Figures 3e and 4c).

In the following we discuss the conformational changes occurring during this reaction, which is more commonly denoted as migratory insertion. On the basis of the optimized geometries of the ethylene hydride complexes (Figures 3 and 4 and Table 5) two important angles serve as approximate reaction coordinates: (i) the angle $\alpha(C_b-Co-H)$ between C_b (the ethylene carbon atom to which the hydrogen migrates), cobalt, and the migrating hydrogen and (ii) the angle $\beta(Co-C_a-C_b)$ between cobalt and the carbon carbon vector of the ethylene moiety.

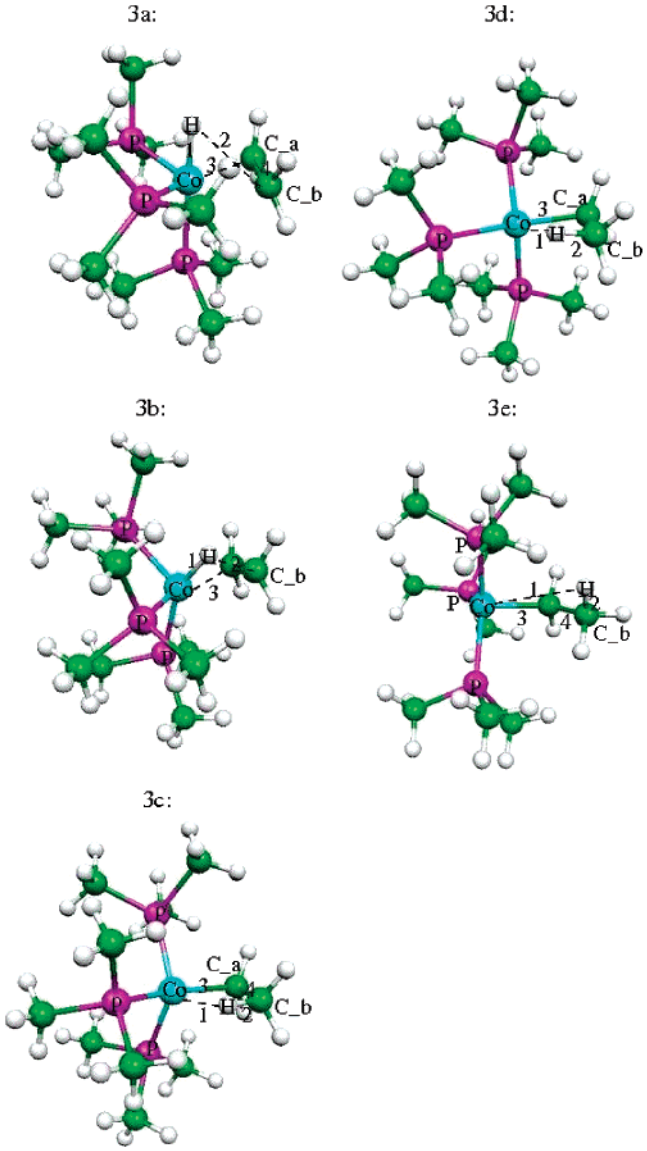

Figure 3. Stationary points with selected structural parameters of the insertion/elimination process for initial structure **1D**.

Table 4. Experimental Activation Parameters ($\Delta H^{\ddagger}$ and $\Delta G^{\ddagger}$ in kcal mol^{-1}, $\Delta S^{\ddagger}$ in cal mol^{-1} K^{-1}) for β-Migratory Insertion

complex	$\Delta H^{\ddagger}$	$\Delta S^{\ddagger}$	$\Delta G^{\ddagger}(T)$	T	ref
$[(C_5R_5)_2Nb(H)(C_2H_4)]$					
R = H			17(1)	318	*a*
R = Me	15(1)	−11(3)			*b*
$[(C_5R_5)_2Nb(H)(C_2H_4)]$					
R = H				347	*a*
R = Me			21(1)	373	*a*
$[(C_5H_5)_2W(H)(C_3H_6)]^+$	23.7(7)	+12(2)			*c*
$[(C_5R_5)\{P(OMe)_3\}Rh(H)(C_2H_4)]^+$					
R = H					*d*
R = Me			12	229	*d*
$[(C_5R_5)(PMe_3)Rh(H)(C_2H_4)]^+$					
R = H					*d*
R = Me			12	224	*d*
$[(C_5R_5)(L)Co(\eta^2\text{-}C_2H_5)]^+$			6−8[f]		*d, e*
R = H, Me; L = $P(OMe)_3$, Me					
$[(PMe_3)_3Co(H)(C_2H_4)]$ (**1**)	16.4(6)	+8(2)			this work

[a] Burger, B. J.; Santarsiero, B. D.; Trimmer, M. S.; Bercaw, J. E. *J. Am. Chem. Soc.* **1988**, *110*, 3134. [b] Doherty, N. M.; Bercaw, J. E. *J. Am. Chem. Soc.* **1985**, *107*, 2670. [c] McNally, J. P.; Cooper, N. J. *Organometallics* **1988**, *7*, 1704. [d] Reference 8g. [e] Reference 8e. [f] Estimated.

Table 5. Geometric Parameters of the Stationary Points (B3LYP/SDD)

initial structure	param[a]	ethylene complex	TS1	agostic ethyl complex	TS2	ethyl complex
1D	$\alpha(C_b-Co-H)$	85	47	29	26	22
	$\beta(Co-C_a-C_b)$	69	72	84	91	107
	$d_1(Co-H)$	1.49	1.52	1.92	2.23	2.97
	$d_2(C_b-H)$	2.40	1.53	1.14	1.12	1.10
	$d_3(Co-C_a)$	2.01	2.01	1.97	1.98	1.99
	$d_4(C_a-C_b)$	1.45	1.47	1.54	1.55	1.56
1E	$\alpha(C_b-Co-H)$	123	51			20
	$\beta(Co-C_a-C_b)$	69	72			117
	$d_1(Co-H)$	1.55	1.51			3.23
	$d_2(C_b-H)$	3.15	1.65			1.10
	$d_3(Co-C_a)$	2.05	2.08			1.98
	$d_4(C_a-C_b)$	1.45	1.43			1.55

[a] The indices at the parameters refer to the distance labels in Figures 3 and 4. Angles are given in deg and distances in Å.

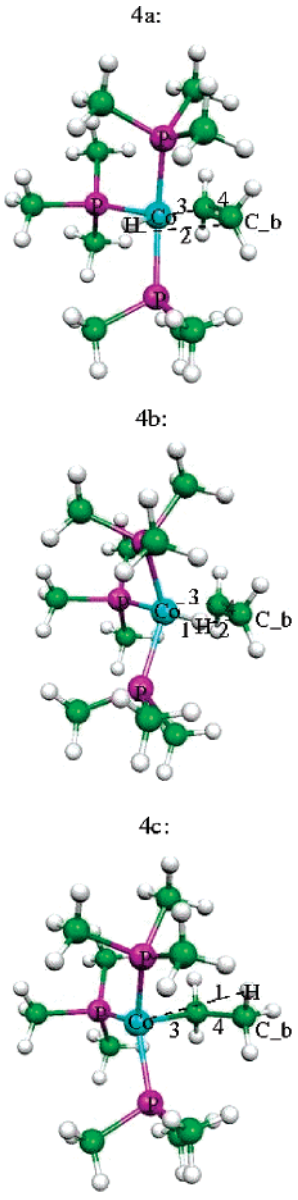

Figure 4. Stationary points with selected structural parameters of the insertion/elimination process for initial structure **1E**.

We found the two different reaction channels (i.e. starting from **1D** and **1E**, respectively) to be fundamentally different as far as the existence of an agostic intermediate is concerned (vide infra). Such an intermediate was found for **1D** as the initial structure (Figure 3c). Starting from **1E**, with the hydride and ethylene ligands both equatorial, no minimum with an agostic structure could be located. The ethyl complexes arising from the two initial geometries are very similar.

In both cases, $\alpha(C_b-Co-H)$ decreases (from 85 to 22° and from 123 to 20°, respectively) while $\beta(Co-C_a-C_b)$ increases (from 69 to 107° and from 69 to 117°, respectively) during the migration process (Table 5). Naturally, the distance $d_1(Co-H)$ between the transition metal and the migrating hydrogen increases. In the ethylene hydride structures, hydrogen is strongly bound to cobalt ($d_1(Co-H)$ = 1.49 and 1.55 Å, respectively). The interaction between these atoms weakens while the interaction between the migrating hydrogen and C_b grows during the insertion. At the endpoint of the reaction, i.e., the ethyl structures, $d_1(Co-H)$ is large (2.97 and 3.23 Å, respectively). Another important quantity is the $d_2(C_b-H)$ distance. It is large for the ethylene structures (2.40 and 3.15 Å, respectively) and decreases to a typical C−H distance of 1.10 Å in the ethyl structures. Our calculated cobalt−carbon bond lengths $d_3(Co-C_a)$ for both the ethylene and ethyl complexes (Table 5) compare well with experimental data reported in the literature ($d(Co-C)$ = 1.91−2.09 Å, $d(Co-C)_{mean}$ = 2.01 Å and $d(Co-C)$ = 1.96−2.04 Å, $d(Co-C)_{mean}$ = 2.01 Å, respectively, for some 20 structurally characterized cobalt ethylene and cobalt ethyl complexes).[28] Obviously, this distance does not change much during the migratory insertion process, when a π type interaction is converted into a cobalt−carbon σ bond ($\Delta d_3 = -0.07$ Å starting from the initial structure **1E** and even less, $\Delta d_3 = -0.02$ Å, from **1D**).

The carbon−carbon distance $d_4(C_a-C_b)$ in the two ethylene structures is rather long (1.45 Å) but agrees reasonably well with the experimental value of 1.43(1) Å in the similar complex $[(PMe_3)_3Co(Ph)(C_2H_4)]$.[12] The considerable increase with respect to the mean value (1.39 Å) taken from the published crystal structures of cobalt ethylene complexes[28] reflects the strong π backbonding from the very electron rich metal center. For the same reason, the CH_2 groups of the coordinated ethylene exhibit a considerable out-of-plane distortion with respect to the C−C bond (dihedral angle of 21° compared to 13° in the complex $[(\eta\text{-}C_5H_5)(PH_3)Rh(H)(C_2H_4)]^+$ [29]). The carbon−carbon interaction is further

(28) Taken from the Cambridge Crystallographic Database (CCDC), Cambridge, U.K., version 5.25, 2004.

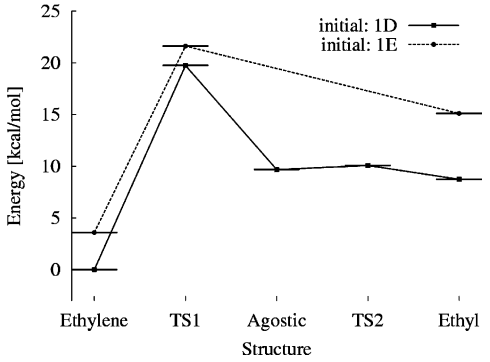

Figure 5. Energies ΔE of the stationary points (B3LYP/SDD) relative to structure **1D**.

Table 6. Energies ΔE of the Stationary Points (B3LYP/SDD) in kcal mol^{-1}

initial structure	ethylene complex	TS1	agostic ethyl complex	TS2	ethyl complex
1D	0	19.7	9.7	10.1	8.7
1E	3.6	21.6			15.1

weakened during the insertion, with a corresponding increase of the distance to 1.56 and 1.55 Å, respectively.

The local energy minimum (Figure 3c) found between the ethylene structure **1D** and the corresponding ethyl complex shows the important characteristics of a β-agostic interaction,[30] notably an acute angle β(Co−C_a−C_b), a moderate distance d_1(Co−H), and a small torsion angle Co−C_a−C_b−H, which places one of the hydrogen atoms of the methyl group more closely to the metal but results in an internally eclipsed conformation of the ethyl substituent (Figure 3e).

Energies of the Stationary Points. The energetics of the migratory insertion processes are given in Table 6 and in the energy level scheme of Figure 5. The energy difference between the transition states resulting from the **1D** and **1E** initial structures is small (1.9 kcal mol^{-1}) for transition state 1 (TS1) compared to the difference of the ethyl structures (6.4 kcal mol^{-1}). The barrier heights between the respective ground state and TS1 are similar in both cases: 19.7 kcal mol^{-1} for **1D** as initial structure and 18.0 kcal mol^{-1} for **1E**. A local energy minimum with an agostic structure (Figure 3c) was only found on starting from structure **1D**, as already mentioned above. Most interestingly, it does not differ much in energy from the resulting ethyl structure. Our calculations even indicate a slightly higher energy (1.0 kcal mol^{-1}) for this agostic intermediate. This is in marked contrast to related systems, where the agostic intermediate was always found at an energy much lower than that of the corresponding ethyl complex (without the β-agostic interaction).[29,31] The barrier between the agostic intermediate and the ethyl structure is also very low (0.40 kcal mol^{-1}).

Potential Energy Profiles. To check the connectivity between the various stationary points discussed above, we also investigated reaction path energy profiles. In the preceding section two approximate reaction coordinates have been pointed out: the angles α(C_b−Co−H) and β(Co−C_a−C_b). Scans along these angles lead to Figure 6 (hydrogen axial) and Figure 7 (hydrogen equatorial). First we focus on the process starting with the axial hydride, as depicted in Figure 6. The left part of the picture corresponds to the ethylene structure **1D** (Figure 3a). The right part of Figure 6 corresponds the ethyl structure (Figure 3e). Note the different angles (α and β) chosen in the two parts of the figure. The cusp in the center, where the coordinate axes merge, represents the agostic structure (Figure 3c). The scan shows the pronounced maximum TS1D between the ethylene and the agostic structure, as well as a very flat maximum TS2E between the agostic and the ethyl structure. We conclude that it costs a great deal of energy to isomerize from the ethylene to the agostic structure (19.7 kcal mol^{-1}) but that the activation energy to isomerize from the agostic structure to the ethyl structure is small (0.4 kcal mol^{-1}). The left panel in Figure 6 also shows that TS1D is a late transition state because the maximum is more on the right side of the panel. For hydrogen equatorial (Figure 7) no agostic structure can be found and thus only one scan leads without a coordinate shift directly from the ethylene structure (Figure 4a and left edge of the scan) to the ethyl structure (Figure 4c and right edge of the scan). Again a prominent late transition state TS1E is found. On comparison of the geometrical data in Table 5 this transition state is similar to TS1D of the hydrogen axial process.

Finally we compare the calculated activation barriers with experiment. For the insertion process, we calculated 19.7 kcal mol^{-1} starting with the global minimum **1D** and 18.0 kcal mol^{-1} when starting with the structure

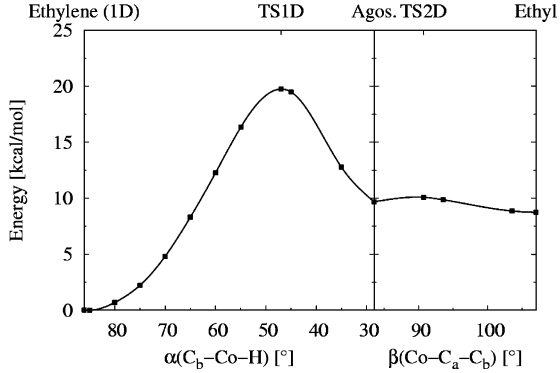

Figure 6. Energy scan (B3LYP/SDD) over approximated reaction coordinates for initial structure **1D**.

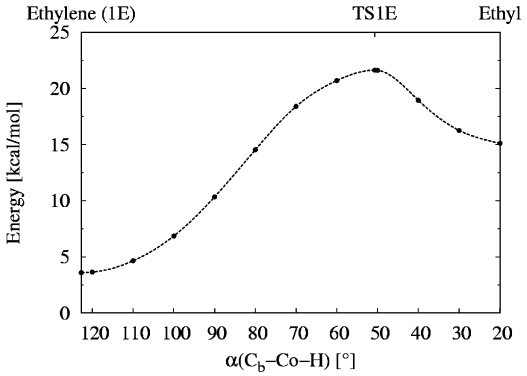

Figure 7. Energy scan (B3LYP/SDD) over an approximated reaction coordinate for initial structure **1E**.

(29) Bittner, M.; Köppel, H. *J. Phys. Chem. A* **2004**, *108*, 11116.
(30) (a) Brookhart, M.; Green, M. L. H. *J. Organomet. Chem.* **1983**, *250*, 395. (b) Brookhart, M.; Green, M. L. H.; Wong, L. L. *Prog. Inorg. Chem.* **1988**, *36*, 1.
(31) (a) Niu, S.; Zarić, S.; Bayse, C. A.; Strout, D. L.; Hall, M. B. *Organometallics* **1998**, *17*, 5139. (b) Han, Y.; Deng, L.; Ziegler, T. *J. Am. Chem. Soc.* **1997**, *119*, 5939.

Table 7. Experimental Activation Parameters ($\Delta H^{\ddagger}$ and $\Delta G^{\ddagger}$ in kcal mol^{-1} and $\Delta S^{\ddagger}$ in cal mol^{-1} K^{-1}) for β-Hydrogen Elimination

complex[a]	$\Delta H^{\ddagger}$	$\Delta S^{\ddagger}$	$\Delta G^{\ddagger}(T)$	T	ref
[(dippp)Pd(η^2-C_2H_5)]$^+$			10(2)	245	*b*
[(NN)Pd(η^2-C_2H_5)]$^+$	6(2)	−5(1)			*c*
[(NN)′Ni(η^2-C_2H_5)]$^+$			14(1)	279	*d*
[(NN)Ni(η^2-C_2H_5)]$^+$			ca. 14	303	*d*

[a] Legend: dippp = 1,3-bis(diisopropylphosphino)propane; (NN) = {2,6-(^{i}Pr)$_2$C$_6$H$_3$}N=C(An)C(An)=N{2,6-(^{i}Pr)$_2$C$_6$H$_3$}; (NN)′ = (2,6-Me$_2$C$_6$H$_3$)N=C(An)C(An)=N(2,6-Me$_2$C$_6$H$_3$). [b] Reference 9g. [c] Reference 9e. [d] Reference 9i.

1E. These numbers agree well with the above results from the magnetization transfer experiments, namely $\Delta H^{\ddagger}$ = 16.4 kcal mol^{-1}. Starting from the ethyl complexes, the activation barriers for β-elimination are found to be 11.0 and 6.5 kcal mol^{-1} (corresponding to the two insertion/elimination pathways studied). For complex **1**, these barriers are not experimentally accessible. However, they compare favorably with results from the literature obtained with related late-transition-metal complexes (Table 7; note that all complexes in the table have agostic ground states).

Another set of calculations, where PMe_3 was replaced by PH_3, did not converge, because the ligands move away from the transition metal for our combination of the method/basis set chosen (B3LYP/SDD). We conclude that the phosphine ligands play a subtle and important role in the stabilization of the molecule. Work is under way to further investigate and quantify their electronic and steric influence.

Conclusion

Comparing our kinetic data for the migratory insertion with the data reported in the literature for late-transition-metal complexes (Table 4), we note that the activation barrier for the neutral cobalt complex **1** is about the same as those found for the cationic rhodium complexes [(C$_5$R$_5$)(PR′$_3$)Rh(H)(C$_2$H$_4$)]$^+$ (R = H, Me; R′ = Me, OMe) and the neutral niobium complexes [(C$_5$R$_5$)$_2$Nb(H)(C$_2$H$_4$)] (R = H, Me). The barriers for the *cationic cobalt* complexes [(C$_5$R$_5$)(PR′$_3$)Co(H)(C$_2$H$_4$)]$^+$ (R = H, Me; R′ = Me, OMe) are substantially smaller, even if the much lower accuracy of those data is taken into account. For the same kind of complex, an increase of the barrier is expected (and found; Table 4) on going down a group in the periodic table. From the available structural evidence it appears to be well established that the less electrophilic the late metal center, the less likely the ethylene hydride is to be agostic.[8,9] Our findings that species (transition states and intermediates) with an agostic metal−H−C interaction become destabilized when the very electron rich (PMe$_3$)$_3$Co moiety is involved (cf. Figures 3, 5, and 6), nicely fits into this trend. Our data also support the idea that the barrier to migratory insertion at a given transition-metal center increases when the metal becomes more electron rich or nucleophilic.[32] Although we cannot completely rule out that our agostic structure (Figure 3c) serves for both insertion pathways (i.e. those starting from **1D** and **1E**), Figure 7 suggests that there may even be cases where an agostic structure is not an intermediate in the migratory insertion/β-hydrogen elimination reaction.[33]

Experimental Section

Complex **1** was prepared as described in the literature.[12]

All NMR measurements were carried out with samples in toluene-d_8, which were flame-sealed under vacuum. A Bruker *Avance* DRX 200 (200 MHz) and a Varian Unity*plus* 400 (400 MHz) spectrometer were used for the magnetization transfer experiments. Kinetic data were acquired at 8−10 different temperatures between −10 and +10 °C. The following protocol was followed at every temperature: a pulse shape of minimal duration was generated with the standard software and hardware facilities of the spectrometers to selectively invert the hydride resonance. With a series of 25−30 experiments, the time evolution of the magnetization of the hydride and ethylene resonances was sampled by application of a nonselective 90° pulse following the selective inversion pulse after a variable time interval. A similar but complementary series of measurements, where the ethylene resonance was selectively inverted, was then carried out.

For a given temperature, the time dependence of the magnetization in the two exchanging sites after inversion of either site was fitted to the appropriate sets of equations derived from the application of the McConnell equations. Fits were carried out for the following (sub)sets of data: the time evolution of magnetization in the two exchanging proton sites i and j (i) after inversion of the hydride resonance or (ii) after inversion of the ethylene resonance and (iii) the combined data from (i) and (ii), i.e. a simultaneous fit of four intensity vs time curves. Several of the nonlinear least-squares fitting routines implemented in the statistical analysis system (SAS)[34] were employed with very similar results. To check the validity of the kinetic equations and the numeric stability of the system, the factors p_{ji}, which account for the different populations of the sites i and j, were included in the fits. These factors came out close to their theoretical values. Comparison of the rate constants obtained from the "forward" (data set (i)) and "backward" (data set (ii)) experiments with those from the combined data set (iii) showed minor discrepancies (Table 2). However, on conversion into energy values, the differences vanished (less than 2σ; Table 3). Eyring plots were calculated for each of the three analyses (i)−(iii). The resulting activation parameters $\Delta H^{\ddagger}$ and $\Delta S^{\ddagger}$ were equal within two standard deviations.

The sample temperature was determined by frequent calibration of the readings of the thermocouples in the standard NMR probes. The conventional methanol thermometer and van Geet's equation[35] was used. The validity of the calibration curves in the range of interest was backed up by and periodically checked with measurements of five different liquid crystal samples. With this method,[36] better than 0.1 K accuracy could be achieved in the temperature range used for our measurements. Temperature stability was excellent (better than 0.2 K), but considerable deviations (up to several K) of the thermocouple readings (i.e. the values used internally by the spectrometer hardware and software) from the measured values were found. To account for systematic errors in the temperature determination, a conservative error of ±0.5 K was assumed for the calculation of the activation parameters. A conventional least-squares procedure was used for the analysis

(32) A theoretical discussion and leading references may be found in ref 4a.

(33) This does not rule out agostic interactions in the transition state.

(34) SAS Statistical Analysis System, Release 8.02, SAS Institute Inc., Cary, NC.

(35) van Geet, A. L. *Anal. Chem*. **1968**, *40*, 2227; **1970**, *42*, 679.

(36) Friebolin, H.; Schilling, G.; Pohl, L. *Org. Magn. Reson*. **1979**, *12*, 569.

(37) Zachmann, H. G. *Mathematik für Chemiker*; Verlag Chemie: Weinheim, Germany, 1972; Chapter XVIII, D. Simple linear regression is clearly not appropriate here.

of the Eyring plots and the calculation of activation parameters.[37] The individual data points were weighted according to the experimental accuracies of the corresponding k and T values.[38] These calculations were carried out with a locally enhanced version of ACTPAR.[39]

Calculational Details. We used a standard DFT method (B3LYP)[40] with the Stuttgart−Dresden basis set (SDD).[41] This method/basis set combination has proven reliable by high-accuracy CCSD(T) calculations on related transition-metal complexes.[29] The nature of the minima and transition states has been verified by frequency calculations (giving zero and one imaginary frequency, respectively). The Gaussian98 program package[42] was used for all calculations.

Acknowledgment. This collaborative work was supported by the Deutsche Forschungsgemeinschaft under the auspices of the Sonderforschungsbereich 623 "Molecular Catalysis". We thank Priv.-Doz. Dr. P. Kirsch, Merck KGA Darmstadt, for the liquid crystal temperature standards and the staff of Varian's NMR Application Laboratory, Darmstadt, Germany, for valuable technical advice.

OM0490740

(38) Weights are not of great importance here, since all data points are of comparable accuracy. This is an advantage of magnetization transfer experiments as compared to methods based on band shape, where accuracy is best around coalescence and quickly drops away from it.

(39) Binsch, G. Universität München, 1969.

(40) Becke, A. D. *J. Chem. Phys.* **1993**, *98*, 1372, 5648.

(41) (a) Dunning, T. H., Jr.; Hay, P. J. In *Modern Theoretical Chemistry*; Schaefer, H. F., III, Ed.; Plenum: New York, 1976; Vol. 3, p 1. (b) Fuentealba, P.; Preuss, P.; Stoll, H.; Lzentpaly, L. v. *Chem. Phys. Lett.* **1989**, *89*, 418. (c) Nicklass, A.; Dolg, M.; Stoll, H.; Preuss, H. *J. Chem. Phys.* **1995**, *102*, 8942.

(42) Frisch, M. J.; Trucks, G. W.; Schlegel, H. B.; Scuseria, G. E.; Robb, M. A.; Cheeseman, J. R.; Zakrzewski, V. G.; Montgomery, J. A., Jr.; Stratmann, R. E.; Burant, J. C.; Dapprich, S.; Millam, J. M.; Daniels, A. D.; Kudin, K. N.; Strain, M. C.; Farkas, O.; Tomasi, J.; Barone, V.; Cossi, M.; Cammi, R.; Mennucci, B.; Pomelli, C.; Adamo, C.; Clifford, S.; Ochterski, J.; Petersson, G. A.; Ayala, P. Y.; Cui, Q.; Morokuma, K.; Malick, D. K.; Rabuck, A. D.; Raghavachari, K.; Foresman, J. B.; Cioslowski, J.; Ortiz, J. V.; Stefanov, B. B.; Liu, G.; Liashenko, A.; Piskorz, P.; Komaromi, I.; Gomperts, R.; Martin, R. L.; Fox, D. J.; Keith, T.; Al-Laham, M. A.; Peng, C. Y.; Nanayakkara, A.; Gonzalez, C.; Challacombe, M.; Gill, P. M. W.; Johnson, B. G.; Chen, W.; Wong, M. W.; Andres, J. L.; Head-Gordon, M.; Replogle, E. S.; Pople, J. A. *Gaussian 98*, revision A.6; Gaussian, Inc.: Pittsburgh, PA, 1998.